

The anterior and posterior biometric characteristics in primary angle-closure disease: Data based on anterior segment optical coherence tomography and swept-source optical coherence tomography

Wenbin Huang^{1,2}, Xingyi Li¹, Xinbo Gao¹, Xiulan Zhang¹

Purpose: Obtaining a better understanding of the pathogenesis of primary angle-closure disease (PACD) still requires studies that provide measurements of anterior and posterior biometric characteristics together and that assess the relationship between them. **Methods:** In total, 201 eyes were enrolled in this cross-sectional study: 50 normal controls, 49 primary angle-closure suspect (PACS), 38 primary angle closure (PAC), and 64 primary angle-closure glaucoma (PACG) eyes. The anterior and posterior structural features were measured by anterior segment optical coherence tomography and swept-source optical coherence tomography. **Results:** All PACD groups had smaller anterior chamber depth (ACD), anterior chamber area (ACA), anterior chamber volume (ACV), angle opening distance at 750 μm from the scleral spur (AOD750), trabecular-iris space area at 750 μm from the scleral spur (TISA750), and angle recess area (ARA), as well as a larger lens vault (LV), than controls (all $P < 0.001$). The PACS and PAC groups had thicker iris thickness at 750 μm from the scleral spur (IT750) than controls ($P = 0.017$ and $P = 0.002$, respectively). Choroidal thickness (CT) was not statistically different among normal, PACS, PAC, and PACG eyes. Univariate and multivariate linear regression analysis revealed a significant association between thinner IT750 and increased CT in PACD eyes ($P = 0.031$, univariate analysis; $P = 0.008$, multivariate analysis). **Conclusion:** Thinner iris thickness was associated with increased CT in PACD eyes; however, the underlying mechanism needs further investigation.

Key words: AS-OCT, ocular biometry, primary angle-closure disease, SS-OCT

Primary angle-closure disease (PACD) is common in Asian populations, with the highest incidence in the Chinese population.^[1,2] PACD has been subdivided into several forms, including primary closed-angle suspect (PACS), primary angle-closure (PAC), acute primary angle-closure glaucoma (APAC), and primary angle-closure glaucoma (PACG).^[3] The biological characteristics of the narrow angle are still one of the most important risk factors for PACD, and its regulation has been proved can affect the onset and progression of glaucoma. However, advances in imaging diagnostic techniques continue to reveal more anatomical risk factors associated with PACD.

Previous studies have reported that PACD has several different biometric factors, including shallow anterior chamber depth (ACD), thick lens, short axis length (AL), and smaller corneal diameter.^[4-6] Recent investigations using anterior segment optical coherence tomography (AS-OCT) have reported a smaller anterior chamber width (ACW), anterior chamber area (ACA), and anterior chamber volume (ACV); increased iris thickness, area, and curvature; changes in iris volume with dilation; and larger lens vaults in association with PACD.^[7,8]

¹Zhongshan Ophthalmic Center, State Key Laboratory of Ophthalmology, Sun Yat-Sen University, Guangzhou, ²Hainan Eye Hospital and Key Laboratory of Ophthalmology, Zhongshan Ophthalmic Center, Sun Yat-sen University, Haikou, People's Republic of China

Correspondence to: Dr. Xiulan Zhang, Director of Clinical Research Center, State Key Laboratory of Ophthalmology, Zhongshan Ophthalmic Center, Sun Yat-sen University, Guangzhou - 510 060, China. 54S Xianlie Road, Guangzhou - 510060, China. E-mail: zhangxl2@mail.sysu.edu.cn

Received: 14-Apr-2020
Accepted: 06-Aug-2020

Revision: 08-Jul-2020
Published: 16-Mar-2021

Access this article online

Website:
www.ijo.in

DOI:
10.4103/ijo.IJO_936_20

Quick Response Code:



Our previous series of studies using enhanced depth imaging optical coherence tomography (EDI-OCT), which focused on posterior ocular biometry,^[9-13] also indicated an association between increased choroidal thickness (CT) and PACD.

However, to better understand the pathogenesis of PACD, we still need to conduct studies to investigate the anterior/posterior structural features of PACD and evaluate the relationship between them. We recently reported concurrent normative values of the anterior/posterior ocular biometric characteristics using AS-OCT and swept-source optical coherence tomography (SS-OCT), and we identified potential relationships between the iris and choroid characteristics in healthy Chinese subjects.^[14] In the present study, we used these same imaging methods to obtain the anterior and posterior biometric characteristics of patients with PACD (including PACS, PAC, and PACG).

Methods

Statement of ethics

This cross-sectional study was conducted from January 2014 to May 2017. The study was approved by the Ethical Review

This is an open access journal, and articles are distributed under the terms of the Creative Commons Attribution-NonCommercial-ShareAlike 4.0 License, which allows others to remix, tweak, and build upon the work non-commercially, as long as appropriate credit is given and the new creations are licensed under the identical terms.

For reprints contact: WKHLRPMedknow_reprints@wolterskluwer.com

Cite this article as: Huang W, Li X, Gao X, Zhang X. The anterior and posterior biometric characteristics in primary angle-closure disease: Data based on anterior segment optical coherence tomography and swept-source optical coherence tomography. Indian J Ophthalmol 2021;69:865-70.

Committee. All participants received detailed explanations of the study and signed informed consent in accordance with the principles embodied in the Helsinki Declaration.

Subjects and enrolment criteria

The study patients were recruited continuously from the glaucoma department. One eye of each subject was included. Subjects were >18 years old with a clear ocular media, and were diagnosed as PACS, PAC, or PACG.^[15,16] Ocular biometry changes caused by acute intraocular pressure (IOP) increases were avoided by excluding patients with APAC. The normal controls were selected from a subgroup of our previous study matched for age.^[14] Control subjects had clear ocular media, open angles, healthy optic nerves, normal visual fields, and no history of IOP exceeding 21 mmHg.

Exclusion criteria for participants enrolled in this study included diabetes, systemic hypertension, or any other systemic diseases; a history of trauma, uveitis, surgery, or any kind of laser therapy; any iris or corneal abnormalities; retinal disease or neuro-ophthalmologic disease; unbearable examination; high myopia or hyperopia with a spherical equivalent refractive error (greater than +3 or -3 diopters); clinically relevant opacities of the optical media, and low-quality images due to unstable fixation or a severe cataract.

Ophthalmic Examination

All subjects underwent a complete ophthalmic evaluation, which included a visual acuity measurement, slit-lamp biomicroscopy, gonioscopy, IOP measurement (Goldmann applanation tonometry), fundus examination, visual field test (SITA standard algorithm with a 24-2 test pattern; Humphrey Visual Field Analyzer II, Carl Zeiss Meditec, Dublin, California, USA), a refractive error examination using an autorefractometer (KR-8900 version 1.07, Topcon Corporation, Tokyo, Japan), and AL measurements using the IOL Master (Carl Zeiss Meditec, Germany).

AS-OCT and SS-OCT measurements

Anterior chamber parameters were measured by AS-OCT (Visante OCT; Carl Zeiss Meditec, Dublin, California, USA) in darkened room conditions (0 lux) by a single operator. The protocol for AS-OCT measurement was the same as described previously.^[14] The images were then processed using the Zhongshan Angle Assessment Program (ZAAP, Guangzhou, China).^[17] The only operation performed on each image was to determine the location of the two scleral spurs. The software then automatically calculated the various anterior chamber parameters. The following parameters were measured: cornea thickness, ACD, ACW, ACA, ACV, pupil diameter (PD), angle opening distance at 750 μm from the scleral spur (AOD750), trabecular-iris space area at 750 μm from the scleral spur (TISA750), angle recess area (ARA), iris thickness at 750 μm from the scleral spur (IT750), iris curvature (ICURV), iris area (IAREA), and lens vault (LV).

Following the AS-OCT measurements, images of the macular region were obtained by SS-OCT (DRI OCT-1; Topcon, Tokyo, Japan). The detailed protocol for SS-OCT measurements was described previously.^[14] A three-dimensional (3D) imaging scan protocol was used for the evaluation of the macular

region. Choroidal and retinal thickness measurements were performed using built-in software (9.12.003.04). A 6 \times 6 mm thickness map of five layers was automatically segmented by the manufacturer's software [Fig. 1]: retinal nerve fiber layer (RNFL), ganglion cell layer plus [GCL+: includes ganglion cell layer and inner plexiform layer (GCL + IPL)], ganglion cell complex [GCC: includes retinal nerve fiber layer, ganglion cell layer, and inner plexiform layer (RNFL + GCL + IPL)], retina (from the inner limiting membrane to the retinal pigment epithelium boundaries), choroid (from the posterior edge of retinal pigment epithelium to the choroid-sclera junction). A 6 mm \times 6 mm scan grid was used for the thickness map, and the mean regional thicknesses of the five layers were calculated for the 36 sectors of the grid.

Statistical analysis

The data were processed and analyzed statistically using SPSS (Version 13.0; SPSS, Chicago, IL). For all tests, a value of $P < 0.05$ was considered significant. The clinical data and measurements were tabulated for all participants and by diagnostic group. Parametric variables were analyzed using analysis of variance (ANOVA) and post hoc LSD tests. Adjusted anterior and posterior parameters among groups were calculated and compared using analysis of covariance (ANCOVA). The association between choroidal thickness and iris parameters was calculated by univariate and multivariate linear regression.

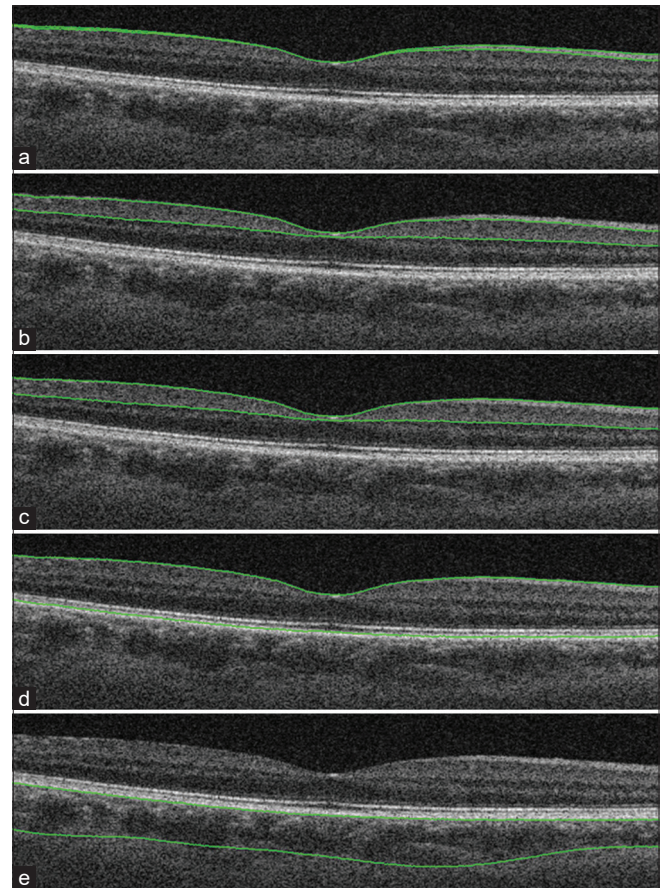


Figure 1: SS-OCT images showing the segmentation of the five layers: retinal nerve fiber layer (a), ganglion cell layer plus (b), ganglion cell complex (c), retina (d), and choroid (e)

Results

In total, 201 subjects (eyes) were enrolled in the study. Of these, 50 were non-glaucoma controls, and 151 were angle-closure eyes classified into one of the following three groups: (1) PACS, 49 eyes; (2) PAC, 38 eyes; and (3) PACG, 64 eyes. The clinical examination data of the four groups are summarized in Table 1. No differences were detected in age and sex among the study groups. As would be expected, AL was significantly longer in normal eyes than in the PACS, PAC, and PACG groups ($P < 0.001$). The PACG group had a higher IOP at imaging when compared with the other groups ($P < 0.001$). The mean numbers of glaucoma medications in the PACG group were 1.6 ± 1.3 (mean \pm SD) and included mainly β -blockers, carbonic anhydrase inhibitors, and α -agonists.

The anterior and posterior ocular biometric characteristics measured by AS-OCT and SS-OCT are also presented in Table 1. After adjusting for age, sex, axial length, IOP, and PD, the AS-OCT parameters for all PACD groups showed smaller ACD, ACA, ACV, AOD750, TISA750, and ARA values and larger LV values when compared with the control eyes (all $P < 0.001$) [Table 2]. The IT750 was significantly thicker in the PACS and PAC

groups than in the normal controls ($P = 0.017$ and $P = 0.002$, respectively) [Table 2]. After adjusting for age, sex, axial length, and IOP, the SS-OCT parameters showed smaller RNFL and GCC thickness for PACG eyes than for the other three groups (all $P < 0.01$) [Table 2]. No significant differences were noted in RNFL, GCL+, GCC, or retina thickness among the normal, PACS, and PAC eyes. The PACG eyes had the thinnest CT, followed by PAC, normal, and PACS eyes; however, no statistical difference was found in CT among these four groups [Table 2].

The relationship between CT and iris thickness was studied by conducting univariate and multivariate linear regression analysis [Table 3]. The univariate regression analysis revealed a significant association between thinner IT750 and increased CT in PACD eyes ($P = 0.031$), but not in normal eyes ($P = 0.396$). The results were the same after adjusting for potential influencing factors (including age, gender, AL, ACW, and PD) ($P = 0.008$ in angle-closure eyes and $P = 0.152$ in normal eyes).

Discussion

Ocular biometry provides the information needed to understand the development of ocular pathologies. Changes

Table 1: Clinical characteristics of the study subjects

Characteristic	Overall	Normal	PACS	PAC	PACG	P*
No. of patients (No. of eyes)	201 (201)	50 (50)	49 (49)	38 (38)	64 (64)	-
Age, y	61.5 (8.9)	58.9 (6.0)	61.4 (7.7)	63.5 (8.7)	62.4 (11.1)	0.069
Sex (female/male)	132/69	29/21	38/11	27/11	38/26	0.112
IOP, mmHg	18.0 (7.1)	16.7 (2.8)	13.7 (3.2)	17.7 (4.0)	23.1 (10.2)	<0.001
AL, mm	22.68 (0.91)	23.32 (0.83)	22.27 (0.77)	22.32 (0.73)	22.70 (0.91)	<0.001
SE, D	1.39 (1.63)	0.86 (1.73)	1.57 (1.31)	2.15 (1.56)	1.20 (1.66)	0.003
ASOCT-anterior segment parameters						
ACD, mm	2.12 (0.38)	2.61 (0.28)	1.94 (0.28)	1.94 (0.22)	1.94 (0.23)	0.001
ACW, mm	11.22 (0.40)	11.57 (0.31)	11.17 (0.34)	11.10 (0.40)	11.05 (0.33)	<0.001
ACA, mm ²	14.76 (3.74)	19.73 (2.75)	13.13 (2.29)	12.82 (1.92)	12.98 (1.98)	<0.001
ACV, mm ³	89.9 (29.7)	129.9 (22.8)	76.3 (16.8)	74.2 (14.5)	76.6 (16.0)	<0.001
PD, mm	4.45 (1.13)	4.59 (0.78)	4.54 (1.31)	4.45 (0.97)	4.25 (1.34)	0.496
ASOCT-mean anterior chamber angle parameters						
AOD750, mm	0.16 (0.12)	0.31 (0.11)	0.08 (0.06)	0.10 (0.06)	0.12 (0.06)	<0.001
TISA750, mm ²	0.07 (0.06)	0.16 (0.06)	0.04 (0.03)	0.03 (0.03)	0.05 (0.04)	<0.001
ARA, mm ²	0.08 (0.07)	0.18 (0.07)	0.05 (0.04)	0.04 (0.03)	0.06 (0.04)	<0.001
ASOCT-iris and lens parameters						
IT750, mm	0.48 (0.09)	0.46 (0.07)	0.50 (0.09)	0.52 (0.09)	0.47 (0.10)	0.032
IAREA, mm ²	1.58 (0.26)	1.53 (0.19)	1.61 (0.25)	1.65 (0.25)	1.53 (0.33)	0.139
ICURV, mm	0.32 (0.13)	0.26 (0.09)	0.39 (0.13)	0.34 (0.12)	0.31 (0.13)	<0.001
LV, μ m	752.9 (282.6)	474.3 (254.8)	935.1 (156.6)	830.1 (215.5)	790.2 (250.5)	<0.001
SSOCT parameters						
RNFL, μ m	30.9 (12.4)	34.7 (7.69)	35.4 (12.0)	34.1 (12.8)	22.4 (11.6)	<0.001
GCL+, μ m	70.6 (20.4)	70.6 (6.21)	75.0 (23.2)	70.1 (6.73)	67.4 (29.1)	0.298
GCC, μ m	99.2 (20.4)	105.3 (12.6)	105.5 (13.4)	104.3 (17.0)	86.2 (25.6)	<0.001
Retina, μ m	256.3 (22.6)	270.2 (14.9)	270.8 (18.9)	272.9 (221.6)	256.3 (27.4)	<0.001
CT, μ m	235.6 (105.2)	246.4 (98.3)	253.3 (101.1)	228.9 (91.5)	217.7 (119.3)	0.279

*P: significance of differences among subgroups: χ^2 test, or ANOVA. Data are expressed as the mean (SD). IOP=Intraocular pressure, AL=Axial length, SE=Spherical equivalent, D=Diopter, ACD=Anterior chamber depth, ACW=Anterior chamber width, ACA=Anterior chamber area, ACV=Anterior chamber volume, PD=Pupil diameter, AOD750=Angle opening distance at 750 μ m from the scleral spur, TISA750=Trabecular-iris space area at 750 μ m from the scleral spur, ARA=Anterior chamber area, IT750=Anterior chamber volume; IAREA=Iris area, ICURV=Iris curvature, LV=Lens vault, RNFL=Macular retinal nerve fiber layer, GCL+ = Ganglion cell layer plus, GCC=Ganglion cell complex, CT=Choroidal thickness, SD=Standard deviation

Table 2: Differences in ASOCT/SSOCT parameters among normal, PACS, PAC, and PACG groups in the adjusted model

Characteristic	Diagnosis	Mean difference (95% CI)	P ^a	P ^b	P ^c
ASOCT parameters¹					
ACD, mm	Normal (ref)	0	-	-	-
	PACS	-0.500 (-0.619, -0.381)	<0.001	-	-
	PAC	-0.507 (-0.629, -0.385)	<0.001	0.907	-
	PACG	-0.511 (-0.634, -0.388)	<0.001	0.868	0.947
ACW, mm	Normal (ref)	0	-	-	-
	PACS	-0.118 (-0.263, 0.027)	0.109	-	-
	PAC	-0.214 (-0.363, -0.065)	0.005	0.157	-
	PACG	-0.342 (-0.488, -0.195)	<0.001	0.003	0.075
ACA, mm ²	Normal (ref)	0	-	-	-
	PACS	-4.903 (-5.928, -3.879)	<0.001	-	-
	PAC	-5.251 (-6.302, -4.200)	<0.001	0.470	-
	PACG	-5.307 (-6.367, -4.247)	<0.001	0.460	0.913
ACV, mm ³	Normal (ref)	0	-	-	-
	PACS	-40.50 (-48.64, -32.36)	<0.001	-	-
	PAC	-43.68 (-52.06, -35.30)	<0.001	0.405	-
	PACG	-45.16 (-53.38, -36.93)	<0.001	0.271	0.713
AOD750, mm	Normal (ref)	0	-	-	-
	PACS	-0.201 (-0.243, -0.159)	<0.001	-	-
	PAC	-0.177 (-0.221, -0.134)	<0.001	0.256	-
	PACG	-0.156 (-0.198, -0.113)	<0.001	0.045	0.314
TISA750, mm ²	Normal (ref)	0	-	-	-
	PACS	-0.110 (-0.131, -0.088)	<0.001	-	-
	PAC	-0.113 (-0.136, -0.091)	<0.001	0.730	-
	PACG	-0.094 (-0.117, -0.070)	<0.001	0.176	0.083
ARA, mm ²	Normal (ref)	0	-	-	-
	PACS	-0.122 (-0.148, -0.096)	<0.001	-	-
	PAC	-0.129 (-0.157, -0.102)	<0.001	0.558	-
	PACG	-0.110 (-0.138, -0.083)	<0.001	0.411	0.163
IT750, mm	Normal (ref)	0	-	-	-
	PACS	0.056 (0.010, 0.102)	0.017	-	-
	PAC	0.076 (0.029, 0.123)	0.002	0.362	-
	PACG	0.019 (-0.030, 0.068)	0.444	0.147	0.020
IAREA, mm ²	Normal (ref)	0	-	-	-
	PACS	0.092 (-0.026, 0.210)	0.125	-	-
	PAC	0.154 (0.032, 0.276)	0.013	0.280	-
	PACG	0.010 (-0.116, 0.137)	0.873	0.212	0.023
ICURV, mm	Normal (ref)	0	-	-	-
	PACS	0.059 (-0.002, 0.120)	0.057	-	-
	PAC	0.009 (-0.054, 0.072)	0.773	0.091	-
	PACG	0.029 (-0.036, 0.095)	0.378	0.375	0.534
LV, μm	Normal (ref)	0	-	-	-
	PACS	288.1 (187.4, 388.8)	<0.001	-	-
	PAC	215.7 (112.6, 318.9)	<0.001	0.126	-
	PACG	251.0 (149.7, 352.3)	<0.001	0.477	0.475
SSOCT parameters²					
RNFL, μm	Normal (ref)	0	-	-	-
	PACS	0.597 (-4.668, 5.862)	0.823	-	-
	PAC	0.559 (-4.851, 5.969)	0.839	0.988	-
	PACG	-10.85 (-16.19, -5.521)	<0.001	<0.001	<0.001

Contd...

Table 2: Contd...

Characteristic	Diagnosis	Mean difference (95% CI)	P ^a	P ^b	P ^c
GCL+, μm	Normal (ref)	0	-	-	-
	PACS	8.315 (-1.670, 18.29)	0.102	-	-
	PAC	2.980 (-7.279, 13.23)	0.567	0.264	-
	PACG	-1.113 (-11.22, 9.011)	0.828	0.077	0.410
GCC, μm	Normal (ref)	0	-	-	-
	PACS	-2.223 (-10.73, 6.290)	0.607	-	-
	PAC	0.115 (-8.633, 8.864)	0.979	0.565	-
	PACG	-14.70 (-23.33, -6.072)	0.001	0.006	0.001
Retina, μm	Normal (ref)	0	-	-	-
	PACS	-2.645 (-12.59, 7.308)	0.601	-	-
	PAC	2.379 (-7.848, 12.60)	0.647	0.292	-
	PACG	-9.723 (-19.81, 0.368)	0.059	0.181	0.015
CT, μm	Normal (ref)	0	-	-	-
	PACS	1.575 (-46.43, 49.58)	0.948	-	-
	PAC	-23.84 (-73.26, 25.57)	0.342	0.268	-
	PACG	-46.24 (-96.07, 3.592)	0.069	0.069	0.357

¹For ASOCT parameters: adjusted for age, sex, axial length, IOP, and PD. ²For SSOCT parameters: adjusted for age, sex, axial length, and IOP. P^aPACS, PAC, PACG vs Normal; P^bPAC, PACG vs PACS; P^cPACG vs PAC

Table 3: Univariate and multivariate linear regression analysis of the association between choroidal thickness and iris thickness

Characteristic	Unadjusted		Adjusted*	
	β (95% CI)	P	β (95% CI)	P
IT750 (per 0.1 mm greater)				
Normal	-17.49(-58.64, 23.65)	0.396	-35.27(-84.08, 13.53)	0.152
PACD (PACS, PAC, PACG)	-23.52(-44.86, -2.198)	0.031	-29.26(-50.69, -7.844)	0.008
Total	-23.23(-41.67, -4.794)	0.014	-23.46(-41.72, -5.204)	0.012

*Adjusted for age, gender, AL, ACW, and PD.

in eye anatomy may lead to visual abnormalities, such as PACD, which is often considered an anatomical disorder.^[4-6] The biometric features of eyes with narrow angles have been studied extensively, especially in the Asian populations.^[18,19] Recent investigations have incorporated improved imaging technologies and have added additional novel factors to the growing list of PACD risk factors, such as greater iris thickness^[20] and choroidal thickness.^[10] However, to date, few studies have attempted to measure the anterior and posterior ocular biometrics together or to evaluate the relationship between these biometrics in PACD. The present study incorporated concurrent AS-OCT and SS-OCT measurements, which provide precise acquisition of images of the anterior and posterior segment of the eye, to achieve a better understanding of the structural features of PACD eyes.

The present study findings confirmed that PACD eyes, after adjusting for potential influencing factors, had smaller ACD, ACA, ACV, AOD750, TISA750, and ARA values and larger LV values when compared with normal control eyes. These biometric features in our series of subjects were similar to those described previously in other Asian subjects.^[19] The PACS and PAC groups, but not the PACG group, had thicker IT750 than was detected in the normal controls. The PACG eyes in the present study had higher IOP compared to the other groups. Thus, a logical hypothesis is that long-term increases in IOP

in PACG eyes would be expected to reduce iris and choroidal blood volume, thereby causing thinning of the iris and choroid.

The posterior segment measurements revealed smaller RNFL and GCC thicknesses in PACG eyes had than in the eyes of the other three groups. No significant differences were noted in RNFL, GCL+, GCC, or retina thicknesses among normal, PACS, and PAC eyes. No statistical difference was found in CT among normal, PACS, PAC, and PACG eyes. These results for CT in the present study differed from those we previously obtained by us using EDI-OCT.^[10] The reasons for this discrepancy may be the use of a different imaging machine and a different measurement model. In our previous study^[10], only nine points of macular CT were measured, whereas a 6 × 6 mm thickness map of the macular CT was acquired in the present study. The use of the average value of the posterior segment CT might have decreased the difference in CT among the four groups. Further studies are needed to explain this discrepancy.

Recent studies have highlighted the role of the choroid and iris in PACD.^[9-13,21] The thick iris accounts for a larger proportion of the anterior chamber volume in the angle recess area. Dilated pupils will make the peripheral iris more pronounced and then more readily able to contact the trabecular meshwork, thereby increasing the risk of angle closure.^[22] Both the iris and choroid are parts of the uvea, so they might influence each other. In

both unadjusted and adjusted models, a significant association was found between the thinner iris thickness and the increased CT in PACD eyes, but the underlying mechanism for this was unclear. Since both the iris and choroid are filled with blood vessels from the ophthalmic artery, we assume that blood flow may play an important role in this association. Thinner iris thickness may increase blood flow resistance in the long posterior ciliary artery (LPCA), which may result in increased blood flow to the short posterior ciliary artery (SPCA). Since both the LPCA and SPCA are derived from the ophthalmic artery, increased blood flow would then lead to choroid thickening.^[23] The dynamic changes in the iris and choroid together may be involved in the pathogenesis of PACD.

Our study has some limitations. One was that the patients were all from the Chinese Han population, so the results may not be applicable to other ethnic groups. Another limitation is that we only measured anatomic ocular parameters using static images. The effects of dynamic factors, such as changes in iris area with pupil dilation^[21] or choroidal changes induced by accommodation,^[24] should not be ignored. However, the assessment of dynamic factors is limited by the difficult nature of the procedures required for image measurement. New algorithms that include dynamic components are required for these measurements. A third limitation is the cross-sectional nature of the study, as this precluded any establishment of temporal or causal relationships. Prospective longitudinal studies are needed to address the cause-and-effect relationships among the dynamic changes in anterior and posterior biometric parameters.

Conclusion

In this study, we used AS-OCT and SS-OCT for concurrent measurement of anterior and posterior biometric parameters in PACD. The relationship between the biometric features of the iris and choroid indicated an association between a thinner iris and an increased CT in PACD eyes; however, the mechanism underlying this association requires further investigation.

Acknowledgements

Thanks Prof. Mingguang He for providing the Zhongshan Angle Assessment Program (ZAAP, Guangzhou, China) for us to analyze the data.

Financial support and sponsorship

The study was funded by Science and Technology Program of Guangzhou, China (201803010066).

Conflicts of interest

There are no conflicts of interest.

References

1. Quigley HA, Broman AT. The number of people with glaucoma worldwide in 2010 and 2020. *Br J Ophthalmol* 2006;90:262-7.
2. Foster PJ, Johnson GJ. Glaucoma in China: How big is the problem? *Br J Ophthalmol* 2001;85:1277-82.
3. Foster PJ, Buhmann R, Quigley HA, Johnson GJ. The definition and classification of glaucoma in prevalence surveys. *Br J Ophthalmol* 2002;86:238-42.
4. Lowe RF. Aetiology of the anatomical basis for primary angle-closure glaucoma. Biometrical comparisons between normal eyes and eyes with primary angle-closure glaucoma. *Br J Ophthalmol* 1970;54:161-9.
5. Sihota R, Lakshmaiah NC, Agarwal HC, Pandey RM, Titiyal JS. Ocular parameters in the subgroups of angle closure glaucoma. *Clin Experiment Ophthalmol* 2000;28:253-8.
6. Alsbirk PH. Primary angle-closure glaucoma. Oculometry, epidemiology, and genetics in a high risk population. *Acta Ophthalmol Suppl* 1976;127:5-31.
7. Nongpiur ME, Ku JY, Aung T. Angle closure glaucoma: A mechanistic review. *Curr Opin Ophthalmol* 2011;22:96-101.
8. Shan J, DeBoer C, Xu BY. Anterior segment optical coherence tomography: Applications for clinical care and scientific research. *Asia Pac J Ophthalmol (Phila)* 2019; Online ahead of print.
9. Chen S, Wang W, Gao X, Li Z, Huang W, Li X, *et al.* Changes in choroidal thickness after trabeculectomy in primary angle closure glaucoma. *Invest Ophthalmol Vis Sci* 2014;55:2608-13.
10. Huang W, Wang W, Gao X, Li X, Li Z, Zhou M, *et al.* Choroidal thickness in the subtypes of angle closure: An EDI-OCT study. *Invest Ophthalmol Vis Sci* 2013;54:7849-53.
11. Wang W, Zhou M, Huang W, Chen S, Ding X, Zhang X. Does acute primary angle-closure cause an increased choroidal thickness? *Invest Ophthalmol Vis Sci* 2013;54:3538-45.
12. Zhou M, Wang W, Ding X, Huang W, Chen S, Laties AM, *et al.* Choroidal thickness in fellow eyes of patients with acute primary angle-closure measured by enhanced depth imaging spectral-domain optical coherence tomography. *Invest Ophthalmol Vis Sci* 2013;54:1971-8.
13. Zhou M, Wang W, Huang W, Gao X, Li Z, Li X, *et al.* Is increased choroidal thickness association with primary angle closure? *Acta Ophthalmol* 2014;92:e514-20.
14. Huang W, Gao X, Li X, Wang J, Chen S, Wang W, *et al.* Anterior and posterior ocular biometry in healthy Chinese subjects: Data based on AS-OCT and SS-OCT. *Plos One* 2015;10:e121740.
15. Foster PJ, Buhmann R, Quigley HA, Johnson GJ. The definition and classification of glaucoma in prevalence surveys. *Br J Ophthalmol* 2002;86:238-42.
16. Ang LP, Aung T, Chew PT. Acute primary angle closure in an Asian population: Long-term outcome of the fellow eye after prophylactic laser peripheral iridotomy. *Ophthalmology* 2000;107:2092-6.
17. Nongpiur ME, He M, Amerasinghe N, Friedman DS, Tay WT, Baskaran M, *et al.* Lens vault, thickness, and position in Chinese subjects with angle closure. *Ophthalmology* 2011;118:474-9.
18. Guzman CP, Gong T, Nongpiur ME, Perera SA, How AC, Lee HK, *et al.* Anterior segment optical coherence tomography parameters in subtypes of primary angle closure. *Invest Ophthalmol Vis Sci* 2013;54:5281-6.
19. Moghimi S, Vahedian Z, Fakhraie G, Ghaffari R, Eslami Y, Jabarvand M, *et al.* Ocular biometry in the subtypes of angle closure: An anterior segment optical coherence tomography study. *Am J Ophthalmol* 2013;155:664-73.
20. Wang B, Sakata LM, Friedman DS, Chan YH, He M, Lavanya R, *et al.* Quantitative iris parameters and association with narrow angles. *Ophthalmology* 2010;117:11-7.
21. Quigley HA, Silver DM, Friedman DS, He M, Plyler RJ, Eberhart CG, *et al.* Iris cross-sectional area decreases with pupil dilation and its dynamic behavior is a risk factor in angle closure. *J Glaucoma* 2009;18:173-9.
22. He M, Wang D, Console JW, Zhang J, Zheng Y, Huang W. Distribution and heritability of iris thickness and pupil size in Chinese: The Guangzhou Twin Eye Study. *Invest Ophthalmol Vis Sci* 2009;50:1593-7.
23. Kim DY, Silverman RH, Chan RV, Khanifar AA, Rondeau M, Lloyd H, *et al.* Measurement of choroidal perfusion and thickness following systemic sildenafil (Viagra(R)). *Acta Ophthalmol* 2013;91:183-8.
24. Woodman EC, Read SA, Collins MJ. Axial length and choroidal thickness changes accompanying prolonged accommodation in myopes and emmetropes. *Vision Res* 2012;72:34-41.